

Received December 31, 2020; reviewed; accepted March 29, 2021

Adsorption mechanism of copper xanthate on pyrite surfaces

Zhengbin Deng ^{1,2,3,4}, Wanli Cheng ^{1,2,3}, Yun Tang ^{1,2,3}, Xiong Tong ^{4,5}, Zhihong Liu ^{1,2,3}

¹ College of Mining, Guizhou University, Guiyang 550025, China;

² National & Local Joint Laboratory of Engineering for Effective Utilization of Regional Mineral Resources from Karst Areas, Guiyang 550025, China

³ Guizhou Key Laboratory of Comprehensive Utilization of Non-metallic Mineral Resources, Guiyang 550025, China

⁴ State Key Laboratory of Complex Nonferrous Metal Resources Clean Utilization, Kunming 650093, China

⁵ Faculty of Land and Resource Engineering, Kunming University of Science and Technology, Kunming 650093, China

Corresponding author: zbindeng@163.com (Zhengbin Deng)

Abstract: The ratio of the hydrophobic to hydrophilic species and their distribution on mineral surfaces significantly influences the floatability of sulfide minerals. Through the flotation test, the influence of different reagents on pyrite flotation was examined. The interaction mechanisms between copper xanthate and pyrite were evaluated using advanced analysis technologies, including contact angle measurements, zeta potential analysis, scanning electron microscopy, energy dispersive spectroscopy, Fourier transform infrared spectroscopy, and X-ray photoelectron spectroscopy. The results show that the butyl xanthate in solution reacts with copper sulfate to form cupric xanthate, increasing the consumption of the collector butyl xanthate and resulting in lower floatability of pyrite. Cupric xanthate can be adsorbed on the pyrite surface through bonding with the sulfur sites. The adsorbed cupric xanthate on the pyrite surface undergoes redox reaction. The cupric xanthate is reduced to cuprous xanthate, and the sulfur on the surface will be oxidized. The adsorption products on the pyrite surface contain both cuprous xanthate and cupric xanthate. As the pH of a solution increases, the absolute value of the zeta potential of pyrite surface increased and the surface contact angle increased. Iron xanthate is also formed on the pyrite surface through a chemical reaction between the xanthate ions and pyrite, oxidation of xanthate ions to dixanthogen also takes place. Cuprous xanthate is the main hydrophobic substance on the pyrite surface, which can change the surface electrical properties and wettability of pyrite, and improve hydrophobicity of pyrite.

Keywords: pyrite, cupric xanthate, cuprous xanthate, adsorption, surfaces

1. Introduction

Pyrite (FeS₂) is the most abundant sulfide mineral in the earth's crust (Mohammadi and Waters, 2016). It is usually associated with minerals that are of economic value, such as sphalerite, galena, chalcopyrite, and precious native metals, such as gold (Chandra et al., 2012). The primary technology for selectively separating pyrite is flotation. This is a physicochemical process that is based on the surface wettability of mineral particles (Bowden and Young, 2016). Flotation recovery is based on the ability of reagents, such as collectors, activators, and depressant, to modify the surface properties of minerals.

Currently, the adsorption of single reagents on pyrite surface has been extensively studied. In the flotation separation of multiple sulfide minerals, pyrite is depressed and then removed as the gangue mineral. Various depressant reagents have been used to control the wettability of pyrite surfaces. Conventionally, some inorganic reagents (inorganic lime, sodium cyanide, sulfur dioxide, potassium dichromate, and calcium hypochlorite.) and organic reagents (dextrin, biopolymers, guar gum, CMC, tannin, starch, chitosan and lignosulfonates.) have been routinely used in the mineral industry as the dominant depressant of pyrite (Liu et al., 2000; Rath et al., 2000; Valdivieso et al., 2004; Bicak et al., 2007;

Huang et al., 2013; Mu et al., 2016; Agheli et al., 2018). In recent years, some new and green depressants (tricarboxystarch, polyglutamic acid) have also been used in pyrite flotation (Khosro et al., 2019a, b; Khosro et al., 2021). Xanthate and copper sulphate are the most commonly used collector and activator in the flotation of pyrite, and have been shown to significantly impact on the flotation recovery. Much effort and significant progress has been made on copper activation and xanthate adsorption in pyrite flotation. In this process of pyrite flotation, copper sulfate is ideally added for the activation of pyrite; then, xanthate is added to make the pyrite surface hydrophobic and to induce flotation. Copper sulfate is adsorbed on pyrite surfaces firstly, and then xanthate adsorption occurs on copper activated pyrite. Copper and xanthate interaction only occur on the pyrite surface, enhancing pyrite floatability.

In the industrial flotation of minerals, the actual dosage of various reagents is higher than the theoretical value. The interaction time between reagents and minerals is short, and its effect is insufficient, a lot of considerable residual reagents in the pulp. Moreover, most concentrators realize the recycling of mineral processing wastewater in the flotation process (Muzenda, 2010), and the residual reagents in the wastewater interact with flotation reagents and significantly influence the flotation process (Deng et al., 2013). Therefore, the intermediate substances such as cupric xanthate, cupric hydroxy xanthates, and cuprous xanthates, which appear when xanthate adsorbs on copper activated pyrite, may be formed in solution although some previous studies also suggest direct surface formation. It has been proved that xanthate in solution reacts with copper sulfate through chemical or electrochemical ways to form colloidal cupric xanthate (Maryan and Matuszak, 1931; Sparrow et al., 1977; Mikhlin et al., 2016).

The adsorption process of flotation reagents on mineral surfaces may occur through different mechanisms, and various species can be produced on surfaces according to these mechanisms. Based on previous studies, cupric xanthate, cupric hydroxy xanthates, and cuprous xanthates as intermediates could appear during xanthate adsorption on copper activated pyrite (Weisener and Gerson, 2000; Deng et al., 2013). Most researchers believe that cuprous xanthate and dixanthate are two typical compounds formed, which determine the hydrophobicity of the pyrite surface and whose action mechanisms are relatively clear (Voigt et al., 1994; Laajalehto et al., 1999; Chang et al., 2003; Chang et al., 2007). Flotation recovery majorly depends on the interaction between various phases on the pyrite surface and the interaction between various chemicals in the water medium (Woods, 1984). However, an investigation of the mineral surface in a flotation pulp in the presence of various reagents is challenging, and the mechanisms of the interfacial processes are not fully understood. This is because of the complex composition of the pulps. A better understanding of the surface chemistry of pyrite may aid to make the industrial froth flotation of pyrite a more efficient process. Therefore, it is of fundamental and practical importance to understanding the interfacial phenomena occurring on pyrite surfaces at the microscale level during the copper xanthate adsorption.

Based on this, this study is motivated by the fact that xanthate reacts with copper sulfate to form cupric xanthate in the pulp. This study demonstrates the hypothesis for cupric xanthate adsorption on pyrite surface. Herein, pyrite samples were conditioned with common flotation reagents, and the flotation behavior of the pyrite was investigated through microflotation experiments. A range of solution and surface analytical techniques (contact angle, zeta potential, scanning electron microscopy and energy dispersive spectrometer, Fourier transform infrared spectroscopy and X-ray photoelectron spectroscopy) were used to identify and quantify the species formed on the pyrite surface. The work provides a certain advance towards the current knowledge on the adsorption mechanism of copper xanthate on pyrite surfaces and supplements the theoretical study understanding of the interaction mechanism of flotation reagents.

2. Materials and methods

2.1. Sample preparation and reagents

The pyrite samples used in this study were obtained from Yiliang Chihong Mine, Yunnan Province, China. The pyrite was separated, crushed and grinded to a particle size of smaller than 74 μm , then dry screened to $-74 + 38 \mu\text{m}$ and $-38 \mu\text{m}$ fractions. The $-74 + 38 \mu\text{m}$ size fraction was used for the SEM-EDS analysis, XPS studies, and microflotation tests. The powder of $-38 \mu\text{m}$ was further ground to $-2 \mu\text{m}$ for the zeta potential measurements and FTIR experimental study. The mineral compositions of pyrite were

analyzed by X-ray diffraction (XRD, Bruker D8, Bruker AXS, Inc., Madison, WI, USA.). The results of X-ray diffraction (Fig. 1) and multi-element chemical analyses (Table 1) confirmed that the purity of the pyrite sample was more than 95%. The pyrite samples contained 46.41% Fe and 53.24% S, which meets the requirement for single minerals.

Table 1. Chemical composition of pure minerals

Composition	Fe	S	Zn	Pb	SiO ₂	Others
Contents/%	46.41	53.24	0.04	0.01	0.17	0.13

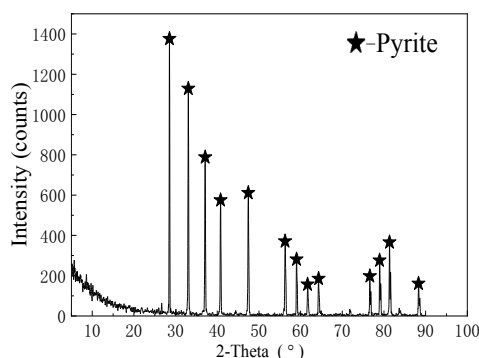


Fig. 1. X-ray diffraction patterns of pyrite

In this study, sodium butyl xanthate (C₅H₉O₅S₂Na, abbreviated SBX) was utilized as the collector, and copper sulphate (CuSO₄) as the activator for pyrite during the conditioning time. All the chemical reagents were of analytical grade. Hydrochloric acid (HCl) and sodium hydroxide (NaOH), which were of analytical grade were utilized as the pH regulators. In addition, distilled water was used in all the experiments. The cupric xanthate was prepared by the method described by Zhang (Zhang et al., 2013). It was prepared by mixing the xanthate solution (1.0×10^{-2} mol/L) and copper sulphate solution (0.5×10^{-3} mol/L). The mixture was stirred vigorously for 10 min and then filtered through a 0.45 μ m membrane filter. Subsequently, it was thoroughly vacuum dried and stored in a desiccator. Fresh cupric xanthate was obtained by washing with hexane.

2.2. Microflotation tests

The flotation performance of pyrite samples was investigated using a 40 mL XFG trough-type laboratory flotation machine (Prospecting Machinery Plant, Jilin, China). The impeller speed was fixed at 1800 r/min. The single mineral flotation test was prepared by adding 2.0 g of minerals to 40 mL of solutions. The pH value was measured by the PHS-3C acidometer built by Leici company (Shanghai, China). The pH of the mineral suspension was adjusted to the desired value by adding NaOH or HCl. After adding the required amounts of reagents, froth flotation was carried out during which a concentrate was collected. The floated and unfloat particles were collected, filtered, and dried. The flotation recovery was calculated based on solid weight distributions between the two products.

2.3. Zeta potential measurements

A Coulter Delsa 440sx zeta potential analyzer was used to determine the zeta potential of the pyrite particles. To produce particles with a size of less than 2 μ m, ceramic agate mortar and pestle were utilized to grind the pyrite sample. After adding 2 g of the sample to 40 mL of distilled water, a given amount of reagents (optimal dosage of microflotation tests) was added at a conditioning time of 3 min. The pulp pH was adjusted using 0.1 mol/L HCl or 0.1 mol/L NaOH. The suspension was left to stand for another 5 min to allow the larger particles to settle. Then, using a syringe, the supernatant was injected into a test electrophoresis tube for measurement. To ensure that accurate results were obtained, measurements of the zeta potential were performed at least five times for each pH value, and then the average value was calculated. The electrolyte utilized in the experiment was 1 mol/L KNO₃ solution, and all measurements were conducted at approximately 25 °C.

2.4. Contact angle measurements

The contact angles of pyrite were measured via the droplet method using contact angle measuring instrument (HARKE-SPCAX3, Beijing Hake test instrument factory, Beijing, China). A cutting machine was used to cut block pyrite into a proper size of approximately $2 \times 2 \times 1$ cm. It was then polished using 60, 400, 800, 1000, and 2000 mesh silicon carbide sandpapers, followed by further polishing with a polishing cloth. The lumps of prepared pyrite sample were immersed in different reagent solutions (optimal dosage of microflotation tests) for 5 min, and the pH was adjusted using diluted HCl and NaOH solutions. Subsequently, the pyrite sample was dried and placed on the test platform. Distilled water (2 μ L) was dropped onto the mineral surface using a syringe. In order to avoid the gravity influence of the droplet, the contact angles were measured 10 s after the droplet falls on the pyrite surface. The average of three contact angle measurements was considered the contact angle of the droplet. All the measurements were performed at approximately 25 °C.

2.5. Scanning electron microscopy with energy dispersive spectrometer (SEM-EDS) analysis

The surface morphology and composition of pyrite before and after treatment with reagents were observed using a field emission scanning electron microscopy (Sigma 300, Carl Zeiss AG) and energy-dispersive X-ray spectrometer (OXFORD X-MaxN). After adding 2 g of the sample to 40 mL of distilled water, a given amount of reagents (optimal dosage of microflotation tests) was added at a conditioning time of 5 min, and the pH was adjusted using diluted HCl and NaOH solutions. After repeated rinsing and filtering, the samples were vacuum dried and used for the measurements. The operating voltage of the SEM was 10 kV, to measure the atomic concentrations of Fe, S, Cu, C, and O on the sample surface.

2.6. Fourier transform infrared spectroscopy (FTIR) analyses

The FTIR spectra of pyrite were recorded in the wavenumber range of 400–4000 cm^{-1} using an FTIR spectrometer (Nicolet iS10, Thermo Fisher Scientific, USA) at room temperature. An ultrasonic treatment of 2 g of pyrite in solution was performed for 5 min to thoroughly clean the mineral surfaces, and then, the cleaned mineral particles were placed in a beaker. Subsequently, a given amount of reagents (optimal dosage of microflotation tests) was added at a conditioning time of 10 min, followed by pH adjustment using diluted HCl and NaOH solutions. After repeated rinsing and filtering, the samples were vacuum dried. Pellets for FTIR spectroscopy analysis were prepared by mixing 1 mg of the pyrite sample to be tested with 100 mg of dry KBr (KBr spectroscopic, Merck).

2.7. X-ray photoelectron spectroscopy (XPS) measurements

XPS was performed using a Versa Probe II spectrometer (PHI 5000, ULVAC-PHI, Japan), utilizing an Al K α X-ray source. After adding 2 g of the sample to 40 mL of distilled water, a given amount of reagents (optimal dosage of microflotation tests) was added at a conditioning time of 5 min. The pH of the suspension was adjusted using 0.1 mol/L HCl or 0.1 mol/L NaOH. After repeated rinsing and filtering, the samples were vacuum dried and used for the measurements. In the experiments, a co-axial neutralization system operated at a filament current and a bias of 1.9 A and 1.2 V, respectively, was used with a charge balance (electron energy) of 3.2 V. The atomic concentrations were calculated using the Casa-XPS software and the Shirley baseline with Kratos library relative sensitivity factors. For all regions, the XPS data were fitted using the Shirley background subtraction and Gaussian-Lorentzian peak profiles. For all other components, charge corrections were made using the C-C binding energy position (284.8 eV) as an internal reference.

3. Results and discussion

3.1. Microflotation test

The influence of different reagents on pyrite flotation was examined through the flotation test. Optimal reagent dosage was determined, as the condition for subsequent tests. The flotation test results are shown in Fig. 2. The flotation experiment results indicate that the recovery rate of pyrite was only 11.2% without reagent. The recovery rate of pyrite substantially improved after adding reagents.

Fig. 2a shows that the recovery rate of pyrite increased with increasing copper sulfate dosage. The maximum recovery rate was 34% when the dosage of copper sulfate was 6 mg/L. Then, the influence of butyl xanthate on the flotation recovery rate of pyrite was investigated. As shown in Fig. 2b, the recovery rate of pyrite increased with increasing butyl xanthate dosage. The maximum recovery rate was 83.4% when the amount of butyl xanthate was 15 mg/L. When the butyl xanthate dosage reached a certain value, the recovery rate plateaued. Fig. 2c shows that the recovery rate of pyrite increased with increasing cupric xanthate dosage. The maximum recovery rate was 55.6% when the dosage was 8 mg/L. Compared to the absence of reagents and presence of copper sulfate, the maximum flotation of pyrite was significantly increased, but it's much lower than that observed when only butyl xanthate was used. The butyl xanthate in solution reacts with copper sulfate forming cupric xanthate, thus increasing the consumption of the collector butyl xanthate and resulting in lower floatability of pyrite. Fig. 2d shows that the pH of the pulp significantly influenced on pyrite flotation when the dosage of flotation reagents was fixed. Under acidic conditions, the pyrite recovery rate changes only slightly with the increasing pH of the slurry. Under alkaline conditions, the pyrite recovery rate shows a downward trend with the increasing pH of the slurry. At a pH range of 8 to 12, pyrite is depressed and the recovery significantly decreases with the increasing pH of the slurry. Under strong alkali conditions, pyrite recovery in cupric xanthate systems decreases slowly.

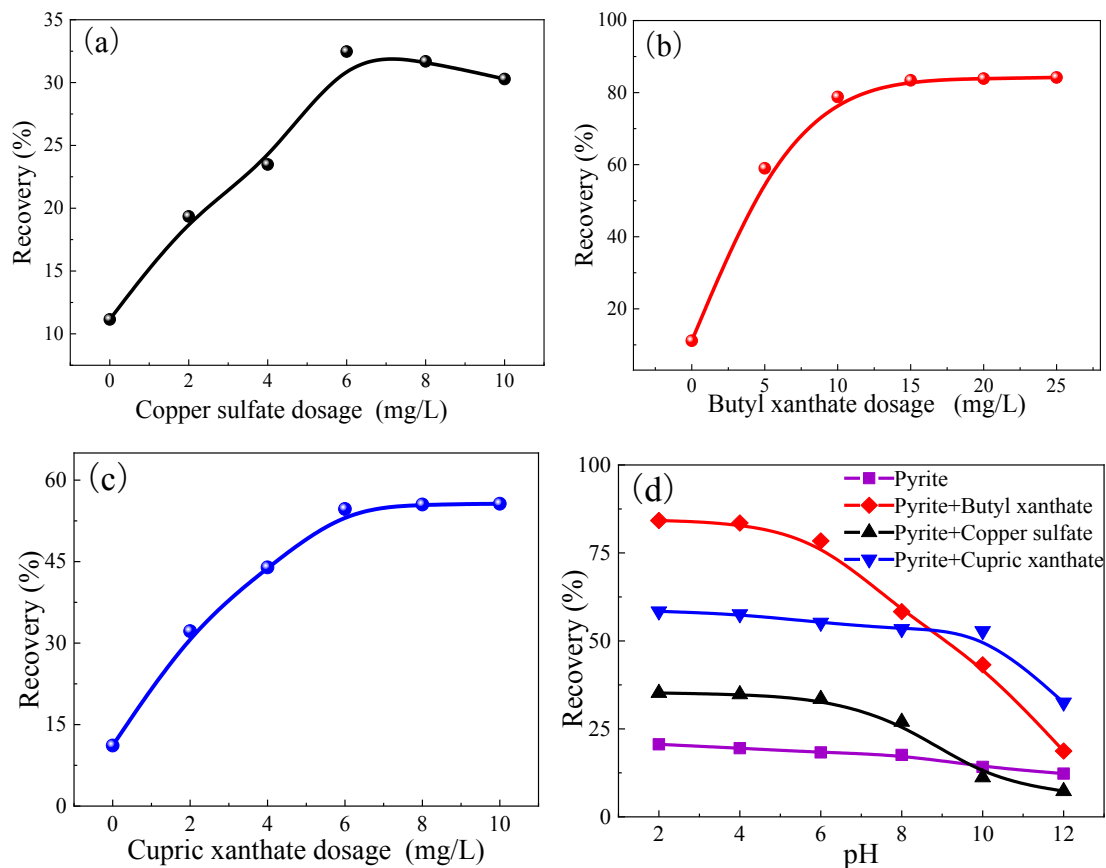


Fig. 2. Effect of flotation reagents dosage and pH on pyrite flotation. (a) Copper sulfate dosage; (b) Butyl xanthate dosage; (c) Cupric xanthate dosage; (d) pH value

3.2. Zeta potential analysis

Zeta potential measurements are widely used to monitor changes in the surface electrical properties of minerals (Li et al., 2018). The surface potential of minerals can be significantly changed by the addition of reagents. The zeta potential of pyrite in the absence and presence of reagents were measured as a function of pH as shown in Fig. 3.

Fig. 3 shows that the isoelectric point (IEP) of pyrite in water was approximately pH 4. The zeta potential on the pyrite surface shifted negatively throughout the pH range. This finding is consistent

with the results reported in the previous literatures (Feng et al., 2012). This finding also indicates that the pyrite sample was oxidized in aqueous solutions exposed in air. After the reagents reacted with pyrite, the IEP of pyrite changed to higher pH values. After adding butyl xanthate, the surface potential of pyrite significantly decreased, reflecting the adsorption of negatively charged xanthate anions (Yin et al., 2018). After adding copper sulfate, the surface potential of pyrite increased and the overall surface potential positively shifted. This is due to the electrostatic adsorption of positively charged Cu^{2+} or CuOH^+ ions on the pyrite surface (Ejtemaei and Nguyen, 2017). When cupric xanthate interacts with pyrite, its surface potential changes, indicating that cupric xanthate can be adsorbed on the pyrite surface and the zeta potential decreases slowly. As the pH increased, the absolute value of the surface potential of pyrite significantly increased.

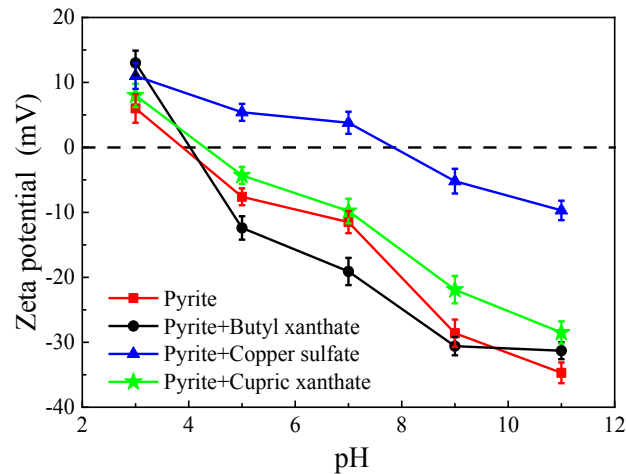


Fig. 3. Zeta potential of pyrite particles as a function of pH

3.3. Contact angle analysis

The wettability of minerals has an important influence on the flotation performance, which is generally characterized by a contact angle (Deng et al., 2017). The wettability of pyrite before and after the action of reagents under different pH values was investigated with contact angle measurements.

In Fig. 4, before the reagents reacted with pyrite, the contact angle of the pyrite surface decreased as the pH values increased, and then slightly increased. The contact angle of the pyrite surface was significantly changed by the reagents. Butyl xanthate adsorbed on pyrite formed dixanthate (López et al., 2005; Peng et al., 2012), which increased the hydrophobicity of the pyrite surface. With the increase in pH values, the pyrite surface promoted the formation of hydrophilic substances, decreasing the contact angle of the pyrite surface (Wang and Forssberg, 1991; Fornasiero and Ralston, 1992). Therefore, the contact angle of pyrite initially decreased and then increased as the pH value increased. After adding

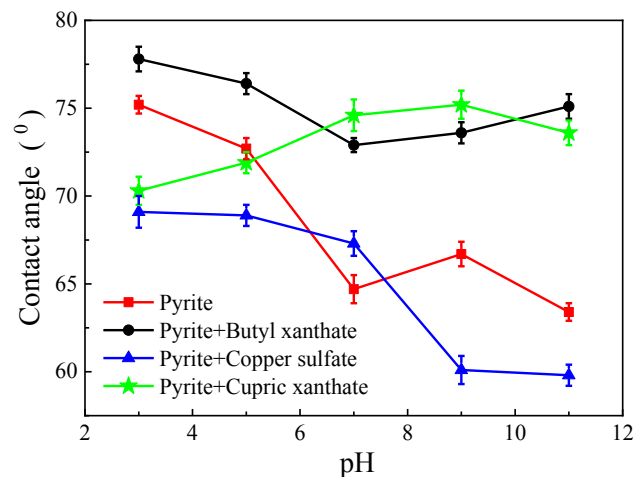


Fig. 4. The contact angle of pyrite as a function of pH

copper sulphate, the contact angle on the pyrite surface decreased as the pH value increased. This is because the pyrite surface tends to form hydrophilic substances, such as $\text{Cu}(\text{OH})_2$, which increases surface hydrophilicity (Weisener and Gerson, 2000). When cupric xanthate is adsorbed on the pyrite surface, the contact angle increases as the pH value increases. The contact angles of pyrite with cupric xanthate under alkaline conditions are greater than those under acidic conditions. At pH 9, a maximum contact angle of 75.2° is observed, and at pH 3, a minimum contact angle of 70.3° is obtained. The result confirms that the pyrite pretreated with cupric xanthate exhibits superior hydrophilicity in the acid solution to that in alkaline solutions.

3.4. SEM-EDS analysis

In Fig. 5, the SEM images of pyrite surfaces after the action of different reagents are presented. Figs. 5 (a) and 5 (b) present the SEM images of the pyrite surface after adsorption of copper sulphate and butyl xanthate. No significant changes were observed on the surface morphologies of the pyrite. In Fig. 5 (c), the surface morphology of pyrite after the action of cupric xanthate is presented. As can be seen from the figure, some flocs appear on the pyrite surface, indicating the formation of new substances and adsorption on the pyrite surface.

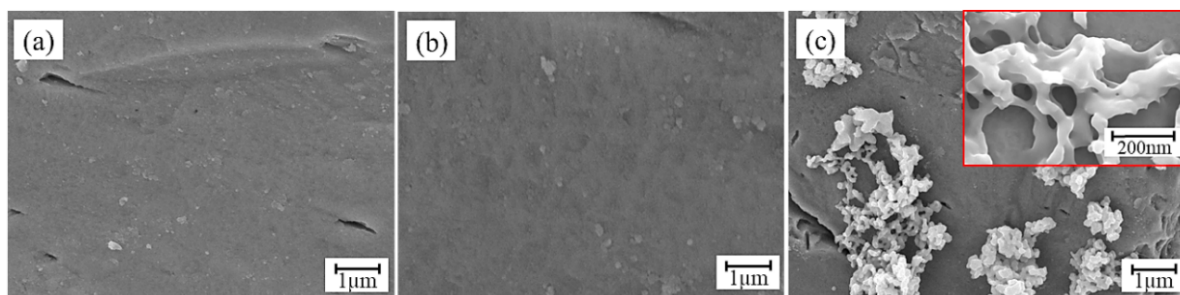


Fig. 5. SEM images of the pyrite surface (a. Pyrite + Copper sulphate; b. Pyrite + Butyl xanthate; c. Pyrite + Cupric xanthate)

As shown in Fig. 6, the EDS point spectrum scanning of flocs and non-flocculated sites demonstrates that in addition to C, O, Fe, and S, Cu is also detected at the adsorption sites, with a weight percentage of 38.14% and an atomic percentage of 16.43%. This further confirms the adsorption of cupric xanthate on the pyrite surface. Previous experiments have demonstrated that the adsorbed product can increase the contact angle of the pyrite surface and the absolute value of the surface potential significantly decreased.

3.5. FTIR Analysis

FTIR spectroscopic measurements were performed to describe the potential mechanism through which reagents are adsorbed on mineral surfaces (Yin et al., 2017). To further investigate the adsorption mechanism of cupric xanthate on the pyrite surfaces, the FTIR spectra of blank pyrite and cupric xanthate samples were determined to understand the interaction pattern. The corresponding results are presented in Fig. 7. The peaks at 1091 and 1416 cm^{-1} in the pyrite spectrum are characteristic peaks of pyrite. The strong and broad band centered at around 3446 cm^{-1} and the peak at 1639 cm^{-1} are attributed to moisture (Zhao et al., 2017; Chai et al., 2018).

After the interaction of pyrite with different reagents, new peaks appeared at different wavenumbers. After interacting with copper sulphate, the characteristic adsorption bands of pyrite showed no obvious changes and no new bands appeared. After butyl xanthate interacted with pyrite, the peaks at 1058 , 1158 , and 1268 cm^{-1} are attributed to the C=S stretching, C-O-C symmetric and asymmetric stretching vibrations in Fe(III)-xanthate. The other set of peaks at 1014 , 1118 , and 1369 cm^{-1} are attributed to the C=S stretching, C-O-C symmetric and asymmetric stretching vibrations of dixanthogen (Wang, 1995; Zhang et al., 2013). After cupric xanthate interacted with pyrite, the peaks at 1143 , and 1201 cm^{-1} are attributed to the C=S stretching, and C-O-C asymmetric stretching vibrations in cupric xanthate (Chandra et al., 2012; Zhang et al., 2013). It can be inferred from the FTIR

spectroscopic results on pyrite-cupric xanthate surface that, both dixanthogen and Fe(III)-xanthate compounds are formed on the surface of pyrite. The peak at 1267 cm^{-1} corresponds to the C-O-C asymmetric stretching vibrations of dixanthogen. The peak at 1039 cm^{-1} is attributed to the C=S stretching vibrations in Fe(III)-xanthate (Leppinen, 1990). This further confirms that cupric xanthate is adsorbed on the pyrite surface.

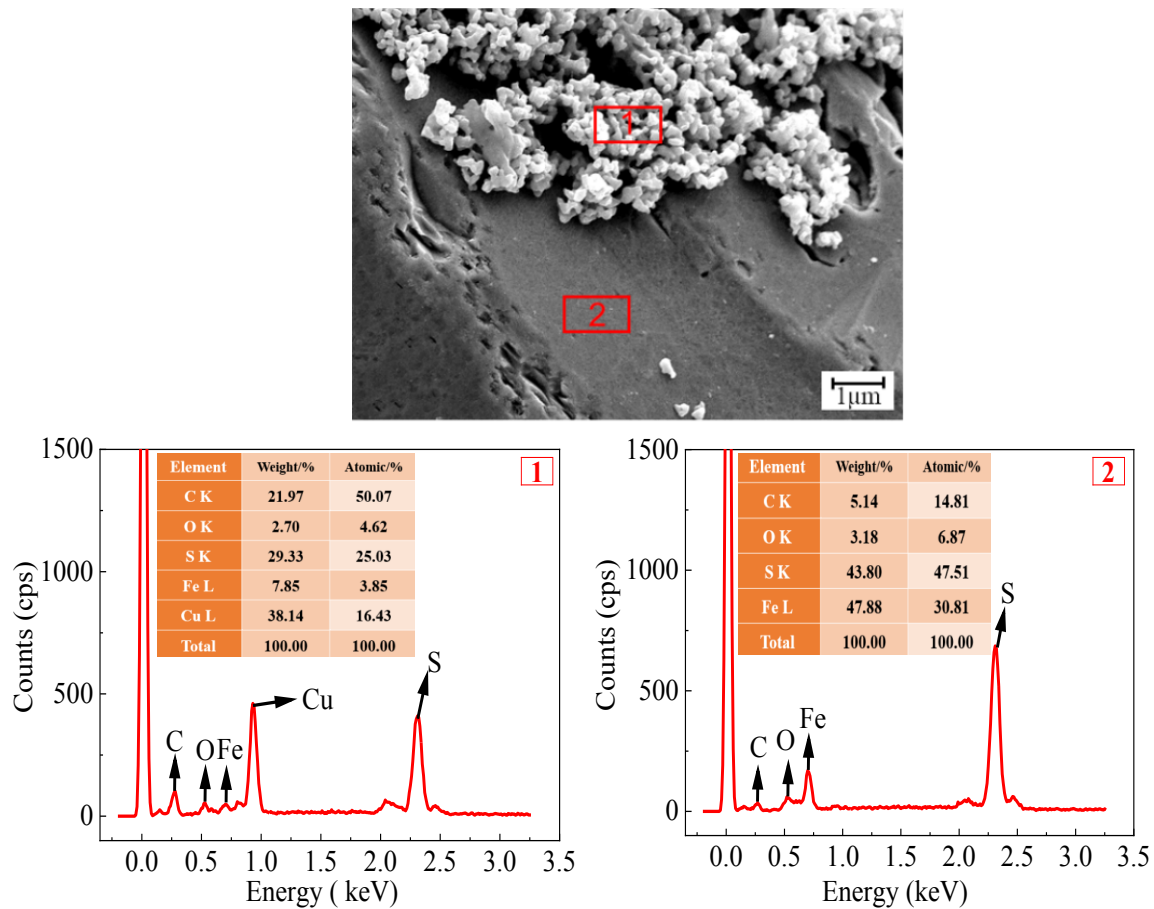


Fig. 6. EDS spectrograms of the pyrite surface after cupric xanthate treatment (1. Surface with flocs, and 2. without flocs)

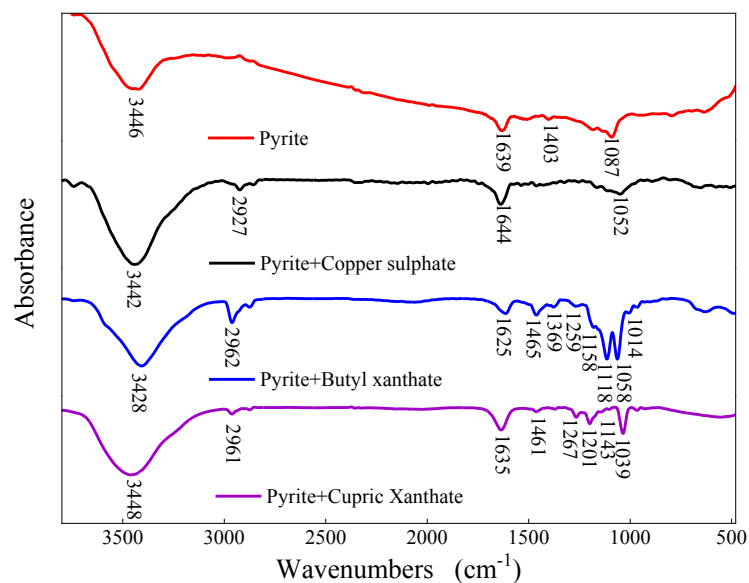


Fig. 7. FTIR spectrum of the pyrite surfaces before and after reagents treatment

3.6. XPS analysis

The results of the contact angle and zeta potential test, SEM-EDS analysis, and FTIR analysis revealed that cupric xanthate can be adsorbed on the pyrite surface. However, the specific mode of action, specific material composition, and effective components were not clear. XPS enables the determination of the compositions and chemical states of newly formed products between reagents and mineral surfaces (Feng et al., 2019; Wang et al., 2020). Therefore, it was employed to explore the interaction mechanism between cupric xanthate and the pyrite surface. In Fig. 8, the Fe2p, S2p, O1s, and C1s spectra collected from pyrite and the samples conditioned with reagents are presented. For clarity, only the S2p_{3/2} and Fe2p_{3/2} components are shown in the pictures.

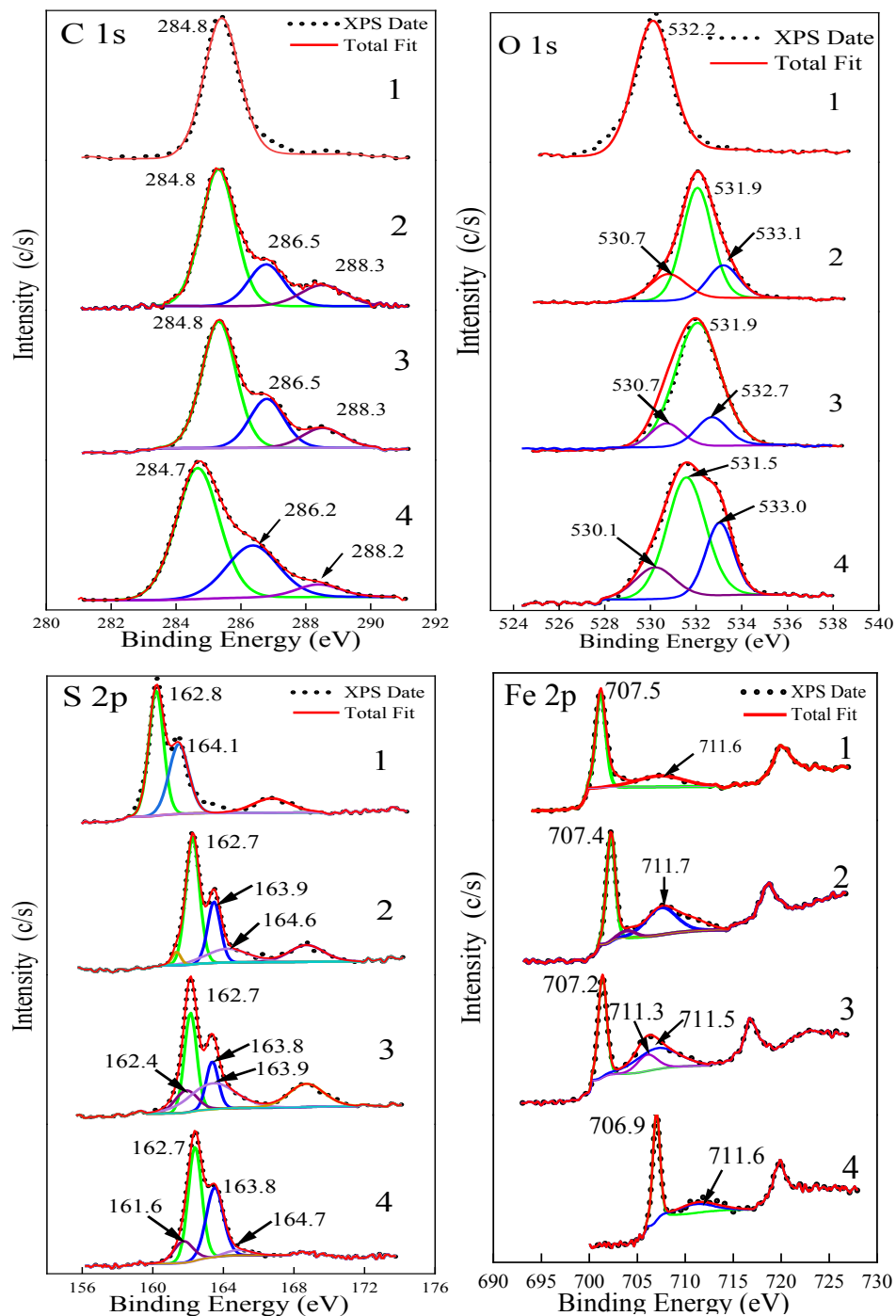


Fig. 8. XPS survey spectra of the C1s, O1s, S2p, and Fe2p regions for pyrite (1. Pyrite; 2. Pyrite + Copper sulphate; 3. Pyrite + Butyl xanthate; 4. Pyrite + Cupric xanthate)

C1s spectra are dominated by the maximum peak at around 284 eV, with two small signals at around 286 and 288 eV, which are generated by the carbon atoms of the contamination layers at different chemical states (Wang et al., 2015; Mikhlin et al., 2016). Unfortunately, the signals of the carbon atoms in the interaction species between cupric xanthate and pyrite cannot be well separated from the contamination signals.

The wide O1s spectrum of pyrite comprises several lines attributable to chemisorbed H₂O, carbonaceous contaminations, OH⁻ groups, and O²⁻ species in ferric oxyhydroxides (Cruz et al., 2001; Boulton et al., 2003; Ejtemaei and Nguyen, 2017). After the interaction between the reagents and pyrite, the O1s signal showed three types of oxygen on the pyrite surface at binding energies of around 530, 531 and 533 eV. The relative amount of the surface carbon and oxygen grows following the cupric xanthate treatment. This is due to the adsorption of cupric xanthate species, which is partial at the least.

The S2p spectra comprise a dominant doublet with S2p_{3/2} peak at around 162.7 eV, which is attributed to S⁻ anions in pyrite, resulting from the Fe-S and S-S bonds (Feng et al., 2012). Other minor peaks are observed at around 164.7 and 163.8 eV, which are attributed to surface polysulfide (S_n²⁻) and monosulfide (S²⁻), respectively. This is interpreted to be the result of S oxidation to S²⁻ or S_n²⁻ (Peng and Grano, 2010; Mu et al., 2016; Rabieh et al., 2016). After the interaction between the reagents and pyrite, the excess of sulfur at 163.8 eV may be ascribed to the S atoms after the cupric xanthate treatment, which is in accordance with the growing contents of C and O at 286.2 and 533.0 eV, respectively. The above analysis of the S2p spectra, reveals that most of the sulfur at 162.5 eV is associated with cupric xanthate. This also indicates that the bulk quantities of C at 286.2 eV and O at 533.0 eV originate from cupric xanthate.

For the Fe2p_{3/2} spectrum, the main peak at around 707 eV could be interpreted as Fe(II) in pyrite, this has been confirmed by other studies (Nesbitt et al., 2000; Murphy and Strongin, 2009). In addition, a peak at around 711 eV is observed, which is typically ascribed to the binding energy of iron oxidation compounds. For simplicity, the iron oxidation species are referred to as Fe(III)-O/OH (Wang et al., 2013). These Fe(III) species could be attributed to Fe(III) oxy or hydroxyl compounds, as the presence of oxides due to the oxidation on the surface was observed at around 530 eV. The latter may have been formed by the immersion of pyrite in the non-acidic solution during conditioning. The FTIR spectroscopic results show that both dixanthogen and Fe(III)-xanthate compounds are formed on the surface of pyrite. This is due to the adsorption of xanthate ions on the pyrite surface through a chemical reaction between the xanthate ions in solution and Fe³⁺ ions on the pyrite surface, resulting in xanthate ions oxidation into dixanthogen (Leppinen, 2013). The adsorption of cupric xanthate on pyrite has no effect on the Fe atomic concentration, thus confirming that there is no ion exchange mechanism. Moreover, it demonstrates that cupric xanthate can be selectively adsorbed on the pyrite surface.

The electronic binding energy of the adsorption system changed after the reaction. Hence, it can be considered that the three reagent molecules can be adsorbed on the pyrite surface. Compared with different reagent systems, the binding energy, peak area, and peak shape of the surface atoms of pyrite are found to significantly change after the adsorption of cupric xanthate. This indicates that cupric xanthate influences the surface atomic state of pyrite. To investigate the formation of adsorbed products on the pyrite surface, the Cu2p spectrum of Cu atom on the pyrite surface was analyzed. The corresponding results are presented in Fig. 9. The Cu2p spectrum detected in the high resolution XPS survey of cupric xanthate adsorption on the pyrite surface is presented. Cu2p_{3/2} was fitted with two peaks, where the main peak at 932.2 eV indicates the formation of cuprous xanthate on the mineral surface, whereas the minor peak at 933.4 eV indicates the formation of cupric xanthate (He et al., 2005; Deng et al., 2013).

Table 2 presents the binding energies and atomic percentages of the C1s, O1s, S2p, Fe2p, and Cu2p spectra collected from the adsorption of cupric xanthate on the pyrite surface. The atomic contents of Cu(I) and Cu(II) are 3.59% and 1.15%, respectively. The adsorption of cupric xanthate on the pyrite surface may be a rapid reaction process, followed by redox reaction, which involves the reduction of cupric xanthate and oxidation of S²⁻ on the surface, together with the partial transfer of S electrons to Cu. Therefore, during the adsorption process, cuprous xanthate and new oxidized sulfur species are produced, which can be adsorbed on the pyrite surface and change the surface electrical properties and wettability of pyrite to varying degrees. It has been reported that the adsorption of Cu xanthate on the

reactive S site is a rapid one step process (Weisener and Gerson, 2000; Zhao et al., 2017). Subsequently, cupric xanthate is reduced to cuprous xanthate, and S on the surface will be oxidized.

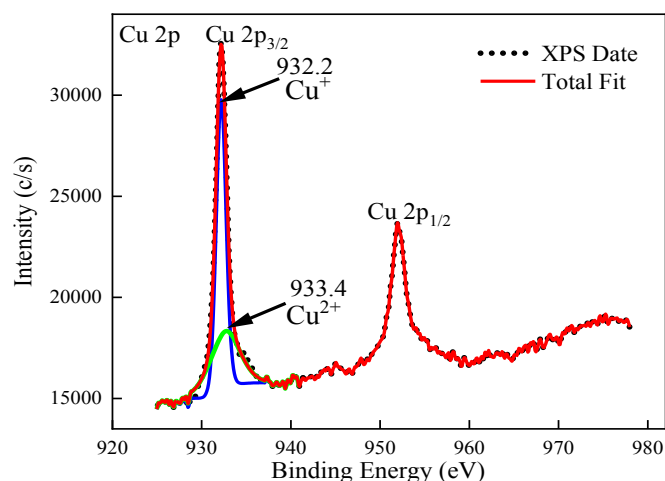


Fig. 9. Cu2p spectra of cupric xanthate adsorbed on the pyrite surface.

Table 2. Binding energy (B.E) and atomic concentrations (atom %) of the elements identified on the pyrite surface with cupric xanthate adsorption

Samples	Comment	Species	B.E (eV)	Atom (%)
	C 1s	C-C (Ref)	284.6	34.14
	C 1s	C-O/C-C*-O	286.2	11.69
	C 1s	C=O	288.2	5.47
	O1s	Oxide	530.1	2.97
	O1s	O-C and OH-	531.5	10.99
	O1s	O=C/C-O*-C	533.0	4.83
Pyrite+ Cupric xanthates	S 2p _{3/2}	S ²⁻ (surface)	161.6	9.62
	S 2p _{3/2}	S(FeS ₂)/S*-C	162.7	7.39
	S 2p _{3/2}	S ²⁻ (activation)	163.8	3.59
	S 2p _{3/2}	S _n ²⁻ /S*-S	164.7	0.82
	Fe 2p _{3/2}	Fe(II)-S	706.9	2.49
	Fe 2p _{3/2}	Fe(III)-O/OH	711.6	1.26
	Cu 2p _{3/2}	Cu(I)	932.2	3.59
	Cu 2p _{3/2}	Cu(II)	933.4	1.15

According to the aforementioned analyses, Fig. 10 presents the reaction process. The outermost sulfur atoms on the surface of pyrite is coordinated with two iron atoms and one sulfur atom. The adsorption of cupric xanthate on the intermediate S site (S₂) does not take place reduction reaction. When cupric xanthate adsorbs on the outermost sulfur atom (S₁ or S₃), electron transfer occurs from sulfur atoms to the cupric xanthate. Then, cupric xanthate is reduced to cuprous xanthate, and S on the surface is oxidized. This is because the low-spin Fe atom of the pyrite surface displays better affinity to the S atom, and the covalency between iron and sulfur atoms is strong (Cui et al., 2020). Owing to the electron enrichment between the two sulfur atoms, the strong electron repulsion, and the tendency to the iron atoms with coordination, electrons are absent around the intermediate sulfur atoms, and the sulfur atoms thus have positive charge (Li et al., 2011). The xanthate ions in the solution chemically reacts with the iron on the surface of the pyrite to oxidize the xanthate ions into dixanthate (Wang, 1995).

The adsorption of cupric xanthate on the pyrite surface produces more cuprous xanthate, rendering the pyrite surface hydrophobic and increasing its floatability. In addition, owing to the adsorption of xanthate ions on the pyrite surface through a chemical reaction between the xanthate ions and pyrite, oxidation of xanthate ions into dixanthogen, both dixanthogen and Fe(III)-xanthate compounds are formed on the surface of pyrite. Above the Fe(III)-xanthate compound layer, dixanthogens and xanthate ions are co-adsorbed probably as multiple layers (Wang and Forssberg, 1991; Chen et al., 2014).

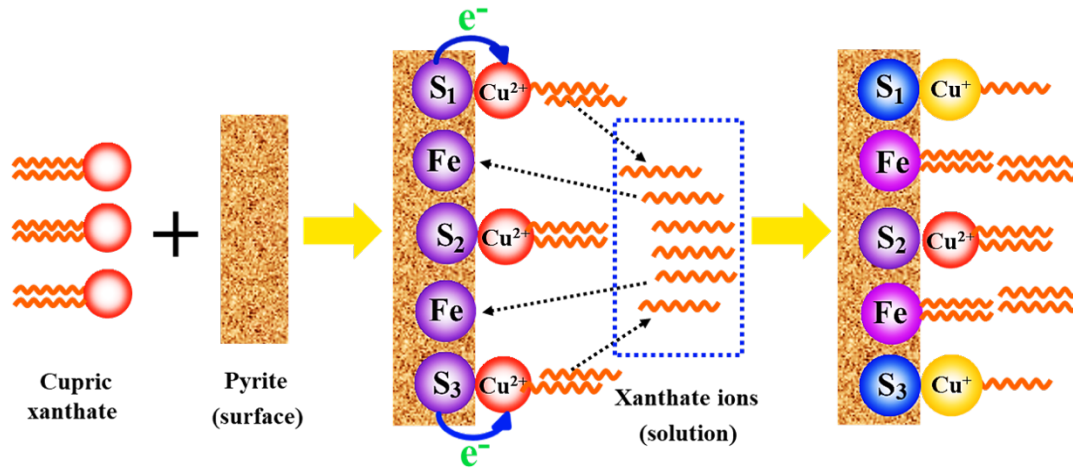


Fig. 10. Schematic diagram of cupric xanthate adsorption on pyrite surfaces

4. Conclusions

In this study, the adsorption mechanism of copper xanthate on pyrite surfaces was investigated. Based on the abovementioned results and discussion, the following main conclusions were drawn:

(1) In the process of pyrite flotation, copper xanthate can be adsorbed on the pyrite surface. The Cu2p X-ray absorption spectrum indicates that the product on the pyrite surface simultaneously contains both cupric xanthate (933.4 eV characteristic peak) and cuprous xanthate (932.2 eV characteristic peak). The contents of Cu(I) and Cu(II) are 3.59% and 1.15%, respectively, indicating that cuprous xanthate is the main adsorbed substance on the pyrite surface.

(2) The adsorption of copper xanthate on the pyrite surface is strong. Following adsorption, the product can change the surface electrical properties and wettability of pyrite. As the pH of a solution increases, the adsorbed product increases the contact angle of the pyrite surface and the absolute value of the surface potential decreased, thus improving the surface hydrophobicity. This is only favorable for the floatability of pyrite in alkaline medium. In actual flotation, the collector will be consumed when cupric xanthate precipitate is formed, reducing the flotation recovery of pyrite.

(3) Cupric xanthate can be adsorbed on specific parts of the pyrite surface. The S2p X-ray absorption spectra revealed that cupric xanthate can be adsorbed on the S sites of the pyrite surface. After the interaction between cupric xanthate and S²⁻ on the surface, the cupric xanthate was reduced to cuprous xanthate, and S²⁻ was oxidized to S⁻ and S_n²⁻. The Fe2p X-ray absorption spectra demonstrated that Fe on the pyrite surface is not involved in the adsorption of copper xanthate and the subsequent reaction process. The FTIR spectroscopic results reveal that both dixanthogen and Fe(III)-xanthate compounds are formed on the pyrite surface. The adsorption of xanthate ions on the pyrite surface occurs through a chemical reaction between the xanthate ions and pyrite, oxidation of xanthate ions to dixanthogen also takes place.

Acknowledgments

This work was financially supported by Open project fund of State Key Laboratory for clean utilization of complex nonferrous metal resources jointly constructed by the Ministry and the province (No. CNMRCUKF1703), National Natural Science Foundation of China (51864010); and the Plan Project of Science and Technology of Guizhou Province of China (Qiankehe Foundation [2017]1404) are gratefully acknowledged.

References

- AGHELL, S., HASSANZADEH, A., HASSAS, B.V., HASANZADEH, M., 2018. *Effect of pyrite content of feed and configuration of locked particles on rougher flotation of copper in low and high pyritic ore types*. Int. J. Min. Sci. Technol. 28, 167-176.
- BOULTON, A., FORNASIERO, D., RALSTON, J., 2003. *Characterisation of sphalerite and pyrite flotation samples by XPS and ToF-SIMS*. Int. J. Miner. Process. 70, 205-219.
- BICAK, O., EKMEKCI, Z., BRADSHAW, D.J., HARRIS, P.J., 2007. *Adsorption of guar gum and CMC on pyrite*. Miner. Eng. 20, 996-1002.
- BOWDEN, J. L., & YOUNG, C. A., 2016. *Xanthate chemisorption at copper and chalcopyrite surfaces*. J. S. Afr. Inst. Min. Metall. 116(6), 503-508.
- CRUZ, R., BERTRAND, V., MONROY, M., IGNACIO GONZÁLEZ., 2001. *Effect of sulfide impurities on the reactivity of pyrite and pyritic concentrates: a multi-tool approach*. Applied Geochemistry. 16, 803-819.
- CHANG, Y.K., CHANG, J.E., CHIANG, L.C., 2003. *Leaching behavior and chemical stability of copper butyl xanthate complex under acidic conditions*. Chemosphere. 52, 1089-1094.
- CUI, W.Y., CHEN, J.H., LI, Y.Q., CHEN, Y., ZHAO, C.H., 2020. *Interactions of xanthate molecule with different mineral surfaces: A comparative study of Fe, Pb and Zn sulfide and oxide minerals with coordination chemistry*. Miner. Eng. 159, 106565.
- CHAI, W., HUANG, Y., PENG, W., HAN, G., CAO, Y., LIU, J., 2018. *Enhanced separation of pyrite from high-sulfur bauxite using 2-mercaptobenzimidazole as chelate collector: Flotation optimization and interaction mechanisms*. Miner. Eng. 129, 93-101.
- CHANG, Y.K., LEU, M.H., CHANG, J.E., LIN, T.F., CHIAN, L.C., SHIH, P.H., CHEN, T.C., 2007. *Combined two-stage xanthate processes for the treatment of copper-containing wastewater*. Eng. Life Sci. 7, 75-80.
- CHEN, J.H., LI, Y.Q., LAN, L.H., GUO, J., 2014. *Interactions of xanthate with pyrite and galena surfaces in the presence and absence of oxygen*. Journal of Industrial & Engineering Chemistry. 20, 268-273.
- CHANDRA, A.P., PUSKAR, L., SIMPSON, D.J., GERSON, A.R., 2012. *Copper and xanthate adsorption onto pyrite surfaces: implications for mineral separation through flotation*. Int. J. Miner. Process. 114, 16-26.
- DENG, M.J., KARPUZOV, D., LIU, Q.X., XU, Z.H., 2013. *Cryo-XPS study of xanthate adsorption on pyrite*. Surface and Interface Analysis. 45, 805-810.
- DENG, M., LIU, Q., XU, Z., 2013. *Impact of gypsum supersaturated water on the uptake of copper and xanthate on sphalerite*. Miner. Eng. 49(Complete), 165-171.
- DENG, W., XU, L.H., TIAN, J., HU, Y.H., HAN, Y.X., 2017. *Flotation and adsorption of a new polysaccharide depressant on pyrite and talc in the presence of a pre-adsorbed xanthate collector*. Minerals. 7, 40.
- EJTEMAEI, M., NGUYEN, A.V., 2017. *Characterisation of sphalerite and pyrite surfaces activated by copper sulphate*. Miner. Eng. 100, 223-232.
- EJTEMAEI, M., NGUYEN, A.V., 2017. *Kinetic studies of amyl xanthate adsorption and bubble attachment to Cu-activated sphalerite and pyrite surfaces*. Miner. Eng. 112, 36-42.
- FENG, B., FENG, Q., LU, Y., 2012. *The effect of lizardite surface characteristics on pyrite flotation*. App. Surf. Sci. 259, 153-158.
- FORNASIERO, D., RALSTON, J., 1992. *Iron hydroxide complexes and their influence on the interaction between ethyl xanthate and pyrite*. J. Colloid Interface Sci. 151, 225-235.
- FENG, Q.C., WEN, S.M., BAI, X., CHANG, W.H., CUI, C.F., ZHAO, W.J., 2019. *Surface modification of smithsonite with ammonia to enhance the formation of sulfidization products and its response to flotation*. Miner. Eng. 137, 1-9.
- HE, S., FORNASIERO, D., SKINNER, W., 2005. *Correlation between copper-activated pyrite flotation and surface species: effect of pulp oxidation potential*. Miner. Eng. 18, 1208-1213.
- HUANG, P., CAO, M., LIU, Q., 2013. *Selective depression of pyrite with chitosan in Pb-Fe sulfide flotation*. Miner. Eng. 46, 45-51.
- KHOSO, S.A., HU, Y.H., LIU, R.Q., TIAN, M.J., SUN, W., GAO, Y., HAN, H.S., GAO, Z.Y., 2019a. *Selective depression of pyrite with a novel functionally modified biopolymer in a Cu-Fe flotation system*. Miner. Eng. 135, 55-63.
- KHOSO, S.A., HU, Y.H., LYU, F., LIU, R.Q., SUN, W., 2019b. *Selective separation of chalcopyrite from pyrite with a novel non-hazardous biodegradable depressant*. Journal of Cleaner Production. 232, 888-897.
- KHOSO, S.A., HU, Y.H., TIAN, M.J., GAO, Z.Y., SUN, W., 2021. *Evaluation of green synthetic depressants for sulfide flotation: Synthesis, characterization and floatation performance to pyrite and chalcopyrite*. Separation and Purification Technology. 259, 118138.

- LEPPINEN J.O., 1990. *FTIR and flotation investigation of the adsorption of ethyl xanthate on activated and non-activated sulfide minerals*. International Journal of Mineral Processing. 30, 245-263.
- LIU, Q., ZHANG, Y., LASKOWSKI, J.S., 2000. *The adsorption of polysaccharides onto mineral surfaces: an acid/base interaction*. Int. J. Miner. Process. 60, 229-245.
- LI, Y.Q., CHEN, J.H., CHEN, Y., GUO, J., 2011. *Density functional theory calculation of surface properties of pyrite (100) with implications for flotation*. Chinese Journal of Nonferrous Metals. 21, 919-926.
- LI, S.K., GU, G.H., QIU, G.Z., CHEN, Z.X., 2018. *Flotation and electrochemical behaviors of chalcopyrite and pyrite in the presence of N-propyl-N'-Ethoxycarbonyl thiourea*. Trans. Nonferrous Metals Soc. China. 28, 1241-1247.
- LAAJALEHTO, K., LEPPINEN, J., KARTIO, I., LAIHO, T., 1999. *XPS and FTIR study of the influence of electrode potential on activation of pyrite by copper or lead*. Colloids Surf. A: Physicochem. Eng. Aspects. 154, 193-199.
- LÓPEZ VALDIVIESO, A., SÁNCHEZ LÓPEZ, A.A., SONG, S., 2005. *On the cathodic reaction coupled with the oxidation of xanthates at the pyrite/aqueous solution interface*. Int. J. Mineral Process. 77, 154-164.
- MUZENDA, E., 2010. *An investigation into the effect of water quality on flotation performance*. Proceedings of World Academy of Science, Engineering and Technology. 70, 237-241.
- MU, Y., PENG, Y., LAUTEN, R.A., 2016. *The mechanism of pyrite depression at acidic pH by lignosulfonate-based biopolymers with different molecular compositions*. Miner. Eng. 92,37-46.
- MIKHLIN, Y., KARACHAROV, A., TOMASHEVICH, Y., SHCHUKAREV, A., 2016. *Cryogenic XPS study of fast-frozen sulfide minerals: flotation-related adsorption of n-butyl xanthate and beyond*. J. Electron. Spectrosc. 206, 65-73.
- MARYAN, MATUSZAK, P., 1931. *Composition of Copper Xanthate*. J. Am. Chem. Soc. 53, 4451-4452.
- MU, Y., PENG, Y., ROLF, A., LAUTEN., 2016. *The depression of pyrite in selective flotation by different reagent systems - A Literature review*. Miner. Eng. 96, 143-156.
- MURPHY, R., STRONGIN, D.R., 2009. *Surface reactivity of pyrite and related sulfides*. Surf. Sci. Rep. 64, 1-45.
- MIKHLIN, Y., VOROBYEV, S., SAIKOVA, S., TOMASHEVICH, Y., FETISOVA, O., KOZLOVA, S., ZHARKOV, S., 2016. *Preparation and characterization of colloidal copper xanthate nanoparticles*. New Journal of Chemistry. 40, 3059-3065.
- MOHAMMADI-JAM, S., WATERS K.E., 2016. *Inverse gas chromatography analysis of minerals: Pyrite wettability*. Miner. Eng. 130-134.
- NESBITT, H.W., SCAINI, M., HOCHST, H., BANCROFT, G.M., SCHAUFUSS, A.G., SZARGAN, R., 2000. *Synchrotron XPS evidence for Fe²⁺-S and Fe³⁺-S surface species on pyrite fracture-surfaces, and their 3D electronic states*. Am. Mineral. 85, 850-857.
- PENG, Y., GRANO, S., 2010. *Effect of grinding media on the activation of pyrite flotation*. Miner. Eng. 23, 600-605.
- PENG, Y., WANG, B., GERSON, A., 2012. *The effect of electrochemical potential on the activation of pyrite by copper and lead ions during grinding*. Int. J. Mineral Process. 102, 141-149.
- RATH, R.K., SUBRAMANIAN, S., PRADEEP, T., 2000. *Surface chemical studies on pyrite in the presence of polysaccharide-based flotation depressants*. J. Colloid Interface Sci. 229, 82-91.
- RABIEH, A., ALBIJANIC, B., EKSTEEN, J.J., 2016. *A review of the effects of grinding media and chemical conditions on the flotation of pyrite in refractory gold operations*. Miner. Eng. 94, 21-28.
- SPARROW, G., POMIANOWSKI, A., LEJA, J., 1977. *Soluble Copper Xanthate Complexes*. Separation Science. 12, 87-102.
- VOIGT, S., SZARGAN, R., SUONINEN, E., 1994. *Interaction of copper (II) ions with pyrite and its influence on ethyl xanthate adsorption*. Surf. Interface Anal. 21, 526-536.
- VALDIVIESO, A.L., CERVANTES, T.C., SONG, S., CABRERA, A.R., LASKOWSKI, J.S., 2004. *Dextrin as a non-toxic depressant for pyrite in flotation with xanthates as collector*. Miner. Eng. 17,1001-1006.
- WOODS, R., 1984. *Woodcock Principles of Mineral Flotation*. Australia Institute of Mining and Metallurgy, Parkville, Victoria, Australia. 91-115.
- WANG X.H., 1995. *Interfacial electrochemistry of pyrite oxidation and flotation. 2: FTIR studies of xanthate adsorption on pyrite surfaces in neutral pH solutions*. Journal of Colloid & Interface ence. 171, 413-428.
- WANG, X.H., FORSSBERG, K.S.E., 1991. *Mechanisms of pyrite flotation with xanthates*. Int. J. Mineral Process. 33, 275-290.
- WEISNER, C., GERSON, A., 2000. *An investigation of the Cu (II) adsorption mechanism on pyrite by ARXPS and SIMS*. Miner. Eng. 13, 1329-1340.

- WANG, J.Y., LIU, Q.X., ZENG, H.B., 2013. *Understanding copper activation and xanthate adsorption on sphalerite by time-of-flight secondary ion mass spectrometry, x-ray photoelectron spectroscopy, and in situ scanning electrochemical microscopy*. J. Phys. Chem. C. 117, 20089-20097.
- WANG, H., WEN, S.M., HAN, G., XU, L., FENG, Q.C., 2020. *Activation mechanism of lead ions in the flotation of sphalerite depressed with zinc sulfate*. Miner. Eng. 146, 106132.
- WANG, J.Y., XIE, L., LIU, Q.X., ZENG, H.B., 2015. *Effects of salinity on xanthate adsorption on sphalerite and bubble-sphalerite interactions*. Miner. Eng. 77, 34-41.
- YIN, Z.G., SUN, W., HU, Y.H., ZHAI, J.H., GUAN, Q.J., 2017. *Evaluation of the replacement of NaCN with depressant mixtures in the separation of copper-molybdenum sulphide ore by flotation*. Sep. Purif. Technol. 173, 9-16.
- YIN, W., XUE, J., LI, D., SUN, Q., YAO, J., HUANG, S., 2018. *Flotation of heavily oxidized pyrite in the presence of fine digenite particles*. Miner. Eng. 115, 142-149.
- ZHANG, Y., CAO, Z., CAO, Y., SUN, C., 2013. *FTIR studies of xanthate adsorption on chalcopyrite, pentlandite and pyrite surfaces*. Journal of Molecular Structure. 1048, 434-440.
- ZHAO, K., YAN, W., WANG, X., HUI, B., GU, G., WANG, H., 2017. *The flotation separation of pyrite from pyrophyllite using oxidized guar gum as depressant*. Int. J. Mineral Process. 161(Complete), 78-82.